Journal of
Nanomedicine & Nanotechnology

Schianti et al., J Nanomed Nanotechol 2013, 4:4
DOI: 10.4172/2157-7439.1000172

Research Article Open Access

Rifampicin Nanoprecipitation using Flow Focusing Microfluidic Device

Juliana N. Schianti[1,2*], Natália N. P. Cerize[2], Adriano M. de Oliveira[2], Silas Derenzo[2], Antônio C. Seabra[1] and Mário R. Góngora-Rubio[2]

[1]Laboratory of Integrated Systems, Polytechnic School , University of São Paulo, Av Prof. Luciano Gualberto, Trav.3, 158, 05508-900, São Paulo, Brazil
[2]Laboratory of Chemical Processes and Particle Technology, Center for Processes and Products Technology, Institute of Technological Research of the State of São Paulo, Av. Prof. Almeida Prado, 532, 05508-901, São Paulo, Brazil

Abstract

We present the nanoprecipitation of rifampicin performed in a microfluidic device as a means to reduce the particle size and enhance the dissolution rate. The microfluidic device was microfabricated in glass substrate with a 45° flow-focusing geometry. The dimensions of the central and side channels are 100 µm and 110 µm in width, respectively, and 85 µm in depth. We analyze the influence of different parameters in the rifampicin particles size, such as: rifampicin concentration, the presence of surfactant, the total fluid flow and solvent to anti-solvent flow rate ratio. The processed rifampicin was evaluated not only in terms of size, but also morphology, crystallinity, thermal characteristics and dissolution rate. We produce particle sizes in a controlled manner with sizes ranging from 100 nm to 1.2 µm. The particles present an amorphous profile and enhanced dissolution rate as compared to commercial raw rifampicin. These results are promising and have enabled us to better understand the rifampicin self-assembly process in microfluidic device.

Keywords: Rifampicin; Nanoprecipitation; Microfluidic device; Amorphous nanoparticles; Flow focusing

Introduction

Microfluidic devices have successfully been applied to produce many kinds of particles in the micro [1-3] and nanoscale range [4,5]. Microfluidics have applications in the pharmaceutical, cosmetic and personal care areas, as well as in chemical processing including paints and coatings, food industry among others [6-8]. In pharmaceutical applications, particularly, microfluidic devices have been applied to synthesize poorly water-soluble drugs with additives in low concentrations, improving the bioavailability by size reduction and morphology changes, while maintaining chemical composition and therapeutic effects [9-12]. Microfluidic devices are utilized to synthesize nanoparticles of organic and inorganic materials such oxides, metals, semiconductors, polymers, including different types of drugs. In the case of pharmaceutical products, there are examples such as liposomes [13-15], niosomes [12], PLGA-PEG copolymer nanoparticles [16] and some poorly soluble drugs that have successfully been produced in microfluidic systems.

The antisolvent precipitation technique is one of the mechanisms applied to obtain nanoparticles and can be improved by using microfluidic devices [17], leading to particles with a smaller nucleation size [18]. Some examples of nanoprecipitation using different kinds of devices can be found in the literature, such as amorphous cefuroxime axetil prepared by nanoprecipitation to enhance the dissolution rate, using a Y-junction micro reactor [19] and a T-junction micro reactor [20]. In that work it was observed that the total fluid flow rate, the anti-solvent to solvent flow rate ratio and the cefuroxime concentration influence the particle sizes. Danazol [21] and calcium atorvastatin [22] are other examples of pharmaceutical ingredients processed in micro reactor, resulting in particles in nanoscale range, with low polidispersity and improved dissolution rate.

Hydrocortisone for ophthalmic delivery was also processed in a commercial micro reactor with Y-junction geometry with good results [23]. The study involved micro reactor with different microchannel diameters and inlet angles. It was observed that smaller microchannels diameters as well as the sharper inlet angles resulted in a reduction of the particle sizes. In the same way, the total flow rate and anti-solvent/solvent ratio affect the particle size. The particle sizes varied from 80 to 450 nm, with the particles having an amorphous profile and the results indicate that the drug dissolution rate is improved if compared with the dissolution rate of raw hydrocortisone. In another work [24], the authors compare the microfluidic nanoprecipitation (a bottom-up method) with the wet milling process (top-down method). It was observed that both methods lead to particles in nanoscale range, improving the bioavailability. However, nanoprecipitation requires low energy consumption and is considered a simple process, while wet milling produces a nanosuspension with more physical stability.

In this work, we present a study of the rifampicin synthesis in a microfluidic device, using the anti-solvent nanoprecipitation process. Rifampicin ($C_{43}H_{58}N_4O_{12}$) is an antibiotic commonly used in Tuberculosis and Hansen disease treatments. However, rifampicin presents a large variability in its bioavailability, due mainly to its two polymorphic forms. Because of its low solubility, rifampicin is administered in high concentrations causing serious side effects [25]. Rifampicin is categorized in class II in the biopharmaceutical classification system (BCS), in which drugs are characterized for their low solubility and high permeability [26,27]. Some methods have been used to increase the rifampicin BCS Class, such as amorphization [28], pH modification and particle size reduction [29] or rifampicin encapsulation in liposomes [30], biodegradable polymers [31]. Although these efforts showed promising results, these techniques utilize additives that are not approved by health organizations and usually cause an increasing in the production costs.

A glass microfluidic device produced by standard micro fabrication

***Corresponding author:** Juliana N. Schianti, Laboratory of Integrated Systems, Polytechnic School , University of São Paulo, Av Prof. Luciano Gualberto, Trav.3, 158, 05508-900, São Paulo, Brazil, Tel: +55 11 3767 4888; E-mail: juliana.schianti@usp.br

Received February 11, 2013; **Accepted** April 22, 2013; **Published** April 25, 2013

Citation: Schianti JN, Cerize NNP, de Oliveira AM, Derenzo S, Seabra AC, et al. (2013) Rifampicin Nanoprecipitation using Flow Focusing Microfluidic Device. J Nanomed Nanotechol 4: 172. doi:10.4172/2157-7439.1000172

processes was used for the study presented here [32,33]. The device has a flow-focusing geometry with 45° angle between the inlets to enhance the diffusion process. The particle sizes and morphology of rifampicin were evaluated while observing the influence of fluid flow, anti-solvent to solvent flow rates, the presence of surfactants and rifampicin concentrations. The nanoparticles were analyzed by techniques of Dynamic Light Scattering (DLS) to measure particle sizes and Field Emission Gun Scanning Electron Microscopy (FEG-SEM) to observe the morphology. Fourier Transform Infrared Spectroscopy analysis was used to observe the chemical composition (FTIR) and X-ray Diffraction (XRD) to analyze the crystallinity. Differential Scanning Calorimetry (DSC) and dissolution tests were used to analyze the rifampicin nanoparticles behavior as compared to raw rifampicin.

Experimental Section

Materials

Rifampicin ($C_{43}H_{58}N_4O_{12}$), Methanol (Sigma-Aldrich), Polyoxyethylene (20) sorbitan monolaurate (Tween 20- Sigma-Aldrich), PBS Buffer Solution pH 7.4 ± 0.1 (Laborclin), soda lime microscope glass slides (76×26×1 mm, Knittel, Germany), acetone, isopropyl alcohol, hydrofluoridric acid solution (39%, General Chemical), hydrochloric acid (38%, General Chemical), UV glue (1201, PIZZANI).

Microfluidic device fabrication

Microscope glass slides were used to obtain the microfluidic devices using standard photolithographic and wet etching procedures. The glasses were patterned with hydrofluoridric acid solution combined with hydrochloric acid to improve the etching process (HF:HCl:H_2O-1:1:3). Chromium films with a thickness of 50 nm, obtained by sputtering, were used as masking material for etching the microchannels. To seal the channels with a cover glass, we used UV glue diluted in 50% pure acetone. Access holes were patterned with diamond burs and brass tubing's used for liquid inlet and outlet was glued with epoxy resin. The flow focusing geometry was patterned to obtain the hydrodynamic flow focusing phenomena. The angle formed between each of the side channels and the main channel is 45° degrees (Figure 1a). The side channels, where the anti-solvent flows, have a width of 110 ± 1µm and the main channel, where the rifampicin solution flows, has 100 ± 1 µm in width. The microchannels have 80 µm + 1 in depth and the diffusion region has 45 + 0.5 mm in length. The glass microfluidic system microfabricated is shown in Figure 1b.

Rifampicin solution and nanoprecipitation process

Rifampicin was dissolved in methanol in three different concentrations, and different flow rates were tested (Q_{RIF}). De-ionized water flow (Q_{WATER}) was used as anti-solvent and was introduced in the side micro channels. The Tween 20 was used as surfactant and we also observed the influence of the flow rate ratio R, which is defined as Q_{WATER}/Q_{RIF}. Syringe pumps, PHD 4400 (Harvard Aparatus), were used for controlling the fluid flows. The flow focusing behavior on the microchannel was observed using an optical microscope (Coleman, XTB-2T).

Statistical data processing using a *two-factor experiment* with repeated measures at central points was applied to study the influence of the parameters settings in the particle size and polydispersity. The parameters are expressed in

Particle size: The size measurement was made in a Dynamic Light Scattering apparatus (Delsa™ Nano C Particle Analyzer, Beckman Coulter). The rifampicin was maintained as a suspension and the DLS analyzer performed six measurements on each sample.

Sample preparation: We filtered and dried the rifampicin nanosuspensions for analysis presented on sequence. Rifampicin nanosuspensions were filtered in a hydrophilic membrane with 0.22 µm in pore (Millipore Ind.) with a vacuum system. The membrane was maintained in a vaccum desiccator per 24 h to dry the sample and obtain the rifampicin powder. We decided also to use a condition without surfactant to observe chemical and physical parameters, and the process conditions: the flow rate ratio between water and rifampicin flow (R) is equal to 10, resulting in particle sizes of 690 nm (Table 1).

Morphology: The nanoparticles morphology was observed by FEG-SEM (Quanta 3D model, FEI).The membrane with nanoparticles was fixed on the FEG-SEM stub using cooper double-sided adhesive tape and sputtered with 20 nm of Au coating. The thickness was defined through the sputtering deposition rate, in our case 5 nm/min.

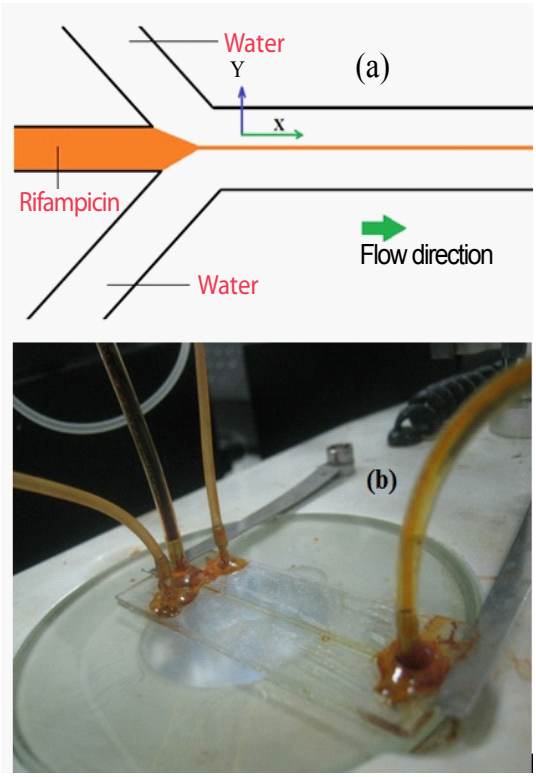

Figure 1: Illustration and photograph of the flow-focusing device used for rifampicin nanoprecipitation. (a) scheme indicating anti-solvent nanoprecipitation process. Rifampicin is focused using water flow on side channels to create a narrow stream in the diffusion region. The solvent (Methanol) diffuses in water (y direction) promoting rifampicin supersaturation in the diffusion region (x direction). (b) Glass microfluidic system, with 110 µm-wide side channels and 100µm-wide central channel, both having 80 µm in depth.

Parameters	-1	0	1
Total Flow Rate – Q (µL/min)	100	150	200
Fluid Flow Ratio - R (Q_{water}/Q_{RIF})	10	30	50
Rifampicin Concentration (mg/mL)	10	30	50
Surfactant (% volume)	0	0.5	1

Table1: Parameters and conditions used in nanoprecipitation experiments.

Chemical composition: The Fourier Transform Infrared Spectroscopy analysis (NICOLET 6700 FTIR, Thermo Scientific) was performed to evaluate the chemical composition of the rifampicin processed in the micro-channel system. FTIR analysis was carried out in a range of 500 to 5000 cm^{-1} with spectral resolution of 2 cm^{-1}, using the potassium bromide pellet method, described elsewhere [34].

Physical characteristics: The crystalline structure was examined using wide X-ray Diffraction (XRD, XRD-6000, and Shimadzu) to observe the crystalline profile changes on the rifampicin processed in microfluidic channels. Data were collected over an angular range from 5 to 50º (2θ) in continuous scan mode using a step size of 0.02°. The generator was set to 40 kV and 30 mA.

Thermal analysis: Thermograms were performed using a Differential Scanning Calorimeter (DSC), Model 822ᵉ (Mettler Toledo). Samples were weighed in aluminum crimped pans. The parameters used for analysis were: heating rate 10°C/min, temperature range 25°C to 300°C with nitrogen purge (100 mL/min) and pan partially covered.

Dissolution rate: Dissolution rate tests were performed in a dissolution apparatus (Shaker 430, Nova Etica). The speed and temperature of the bath were set at 100 rpm and 37.0°C ± 0.5°C, respectively. A PBS buffer solution with pH of 7.4 was employed as the dissolution medium. Rifampicin samples, both the commercial and the rifampicin nanoparticles, with 6 mg of mass were added to different vessels containing 100 mL of the dissolution medium. A 3 mL aliquot was taken each time at specific time intervals (2, 5, 10, 15, 20, 25, 30, 35, 40, 45, 50, 60, 90, 120 and 180 minutes) and the concentration of samples was obtained by absorbance measurement in an UV spectrophotometer (U-2000, UV Hitachi) at 333 nm.

As a reference, a sample of raw rifampicin (pure drug) was characterized with the same techniques applied to the rifampicin nanoparticle obtained in microfluidic process (FEG-SEM, FTIR, DSC, XRD and dissolution tests) and the results are discussed below. Commercial Rifampicin was diluted with distilled water and filtered in the same way as the nanoparticles. The initial average size of raw rifampicin was 42 µm.

Results and Discussion

Flow focusing and particle sizes

Figure 2, presents the images of microfluidic device in two different flow rate ratios and their respective particle size measurement. For the examples shown below, the initial rifampicin concentration is 50 mg/mL. In (a) the anti-solvent to solvent ratio R is equal to 10, resulting in a 690 nm rifampicin particle size. In (b), the ratio is equal to 50 and resulted in a 160 nm rifampicin particle size. In these examples, we fixed the water flow rate, Q_{WATER}, to 200 µL/min. As expected, for higher R values, small particle sizes are obtained. However, this microfluidic system allows a maximum R value of 50, since for higher values, the flow focusing is no longer achieved.

Factorial analysis

Under the conditions used in this work, it was possible to obtain rifampicin nanoparticles in a range from 100 nm to 1120 nm and polidispersity below 0.3. In figure 3, we can see the surface analysis response showing the influence on the particle size of each selected parameters used in the experiments. It is possible to observe that the increase in total fluid flow combined with the increase of Q_{WATER}/Q_{RIF} ratio causes a reduction in the particle size.

Higher rifampicin concentration results in larger particles, while higher surfactant concentration reduces the particle sizes. By varying the concentration of surfactant in the range of 0-1% by volume of water, there is a reduction in particle size from 800 nm to 250 nm approximately, considering an anti-solvent to solvent flow ratio of

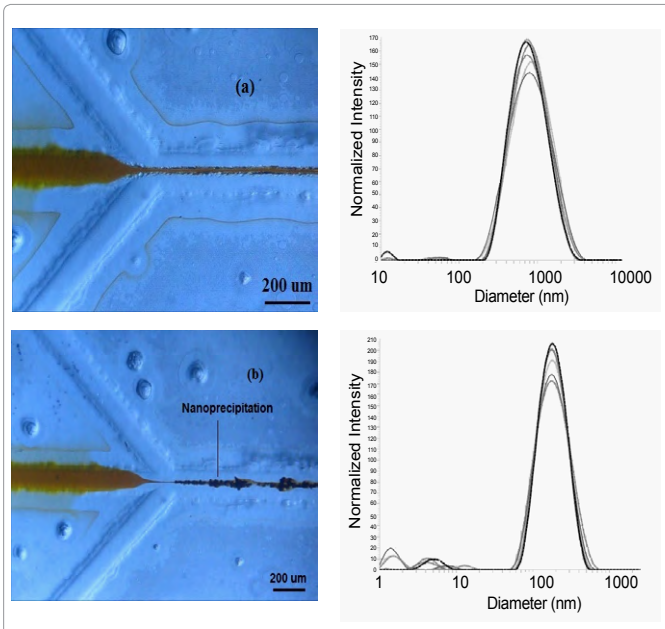

Figure 2: Optical Microscope images of rifampicin solution in microfluidic flow focusing with respective particle size measurement (DLS): (a) the flow rate ratio between water and rifampicin flow (R) is equal to 10, resulting in particle sizes of 690 nm. (b) R is equal to 50, resulting in particle sizes of 160 nm. In these examples the water flow was maintained at 200 µL/min, and rifampicin concentration was 50 mg/mL.

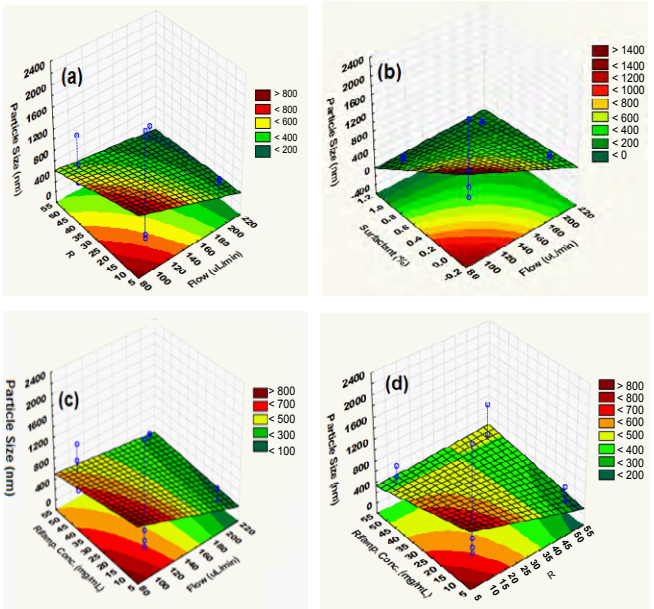

Figure 3: Surface area graphs showing the parameter's effects on the particle size: (a) water flow and flow rate ratio (R); (b) surfactant and water flow; (c) rifampicin concentration and water flow and (d) rifampicin concentration and flow rate ratio (R).

50 and water fluid flow of 200 µL/min. The total water flow does not present statistically significant influence in the final particle sizes, as can be seen in the histograms shown in figure 4, but provides a larger final volume of suspension in a given period of time; we thus work with higher fluid flow rate (200 µL/min). The histogram was done based on the data obtained in our factorial experiments.

Morphology

Figure 5 shows micrographs of rifampicin nanoparticles obtained with a FEG-SEM. In this analysis the rifampicin was maintained in the membrane used previously to filter rifampicin. In figure 5a, a micrograph of raw rifampicin is shown and in figure 5b rifampicin processed in microfluidic devices is presented (measured size of 250 nm). For this analysis we utilized Rifampicin in high initial concentration (50 mg/mL), and the microfluidic system was operated with a water flow rate (Q_{water}) of 200 µL/min and R of 50. We observed that the particles obtained from the microfluidic process have a spherical shape as compared to commercial raw rifampicin.

Chemical composition

FTIR analysis was performed to evaluate the chemical composition of the raw rifampicin and the microfluidic processed rifampicin nanoparticles. The corresponding FTIR spectra are presented in figure 6. The FT-IR spectra curves suggest that there was no chemical composition change, because rifampicin nanoparticles have the same absorption peaks as raw rifampicin.

X-ray diffraction analysis

In figure 7, a XRD profile is presented comparing the raw rifampicin with rifampicin processed in the microfluidic device. Raw rifampicin shows characteristic peaks at 19.50°, 14.35° and 13.65°. As presented in the article by Agrawal et al. [27], commercial rifampicin is usually a mixture of crystal forms I (presenting peaks at 14.35° and 13.65°) and II (19.5°), and amorphous material. Observing the curve for rifampicin processed in microfluidic system, the absence of peaks is verified, revealing that this material has a significant reduction in crystallinity and is mostly amorphous. In many pharmaceuticals applications, size reduction is combined with crystal amorphization, since amorphous particles have higher solubility compared to crystalline particles, even for particles on nanoscale range [34].

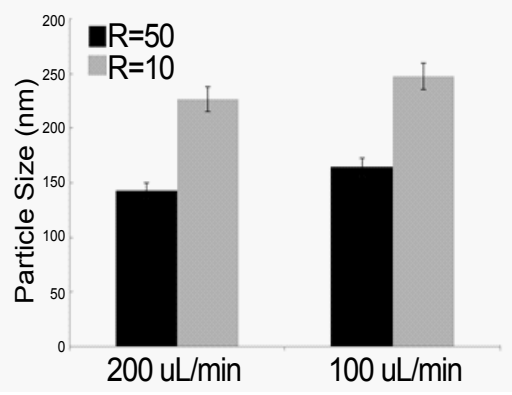

Figure 4: Histogram showing the effect of water flow (Qwater) combined with flow ratio R (Q_{WATER}/Q_{RIF}) on the rifampicin particle sizes. The water flows (Qwater) used in our experiments do not provide significant differences in particle sizes (around 50 nm). The ratio between water and rifampicin flow, combined with rifampicin initial concentration causes a relevant influence on the particle sizes.

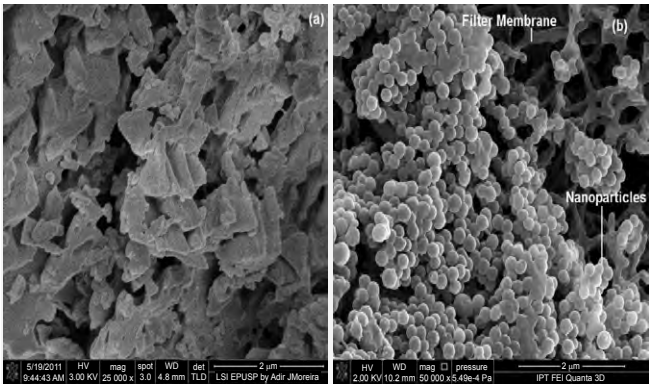

Figure 5: SEM-FEG analyses of rifampicin: (a) raw rifampicin was diluted (0.002 kg) in water and filtered for the analysis and in (b) rifampicin nanoparticles obtained by nanoprecipitation in the microfluidic system using 200 µL/min of water flow, rifampicin concentration of 50 mg/mL and ratio between phases (R) equal 50.

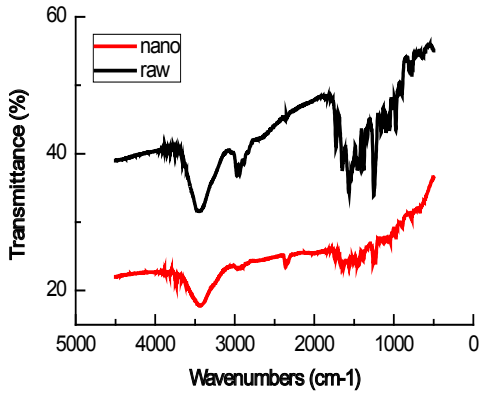

Figure 6: FTIR spectra of (a) raw rifampicin and (b) rifampicin nanoparticles. Raw rifampicin presents an absorption peak in 3480 cm^{-1}, and rifampicin nanoparticles maintained the same absorption peak, indicating there are no changes in chemical composition after microfluidic synthesis.

Thermal analysis

The DSC profile of raw rifampicin showed two peaks at 190°C and 260°C, which correspond to the melting point and decomposition of the raw rifampicin, respectively (Figure 8a). In contrast, in the DSC thermal profile of rifampicin nanoparticles, we can see slight bands confirming the amorphous state of these particles (Figure 8b). Although we could observe some noises on the DSC profile of rifampicin nano, we could see that there are marked differences between DSC profiles. The XRD analysis presented before helped us maintain this argument.

Dissolution tests

The dissolution profiles of raw rifampicin and the nanoparticles (690 nm) in phosphate buffer solution are compared in figure 9. In ten minutes, the rifampicin nanoparticles reached 50% drug dissolution against 30% of the raw rifampicin in the same period. The green line on the graphic highlights the period of 45 minutes stipulated by US

Pharmacopeia a for rifampicin dissolution tests [35]. In this point, we observed that 80% of nano rifampicin is dissolved in contrast of 60% of raw rifampicin. The results indicate that rifampicin nanoparticles provide an improved dissolution rate compared to raw rifampicin.

Conclusion

In this work, a glass micro fluidic device was employed to produce rifampicin nano-suspension with a relative control over particle size and morphology. The nanoprecipitation process in our device leads to rifampicin nanoparticles with sizes in a range varying from 100 nm up to 1120 nm. When comparing processed with unprocessed rifampicin, we observed that the chemical characteristics were maintained, as can be seen from the FTIR analysis, however, the particles morphology becomes amorphous. The change to amorphous profile was confirmed by DSC and XRD analysis. The dissolution profile was evaluated in a buffer solution, and we observed that rifampicin nanoparticle has the dissolution rate enhanced compared to raw rifampicin. In conclusion, the rifampicin nano-precipitation in micro fluidic device offers a continuous controlled process to obtain rifampicin nanoparticles.

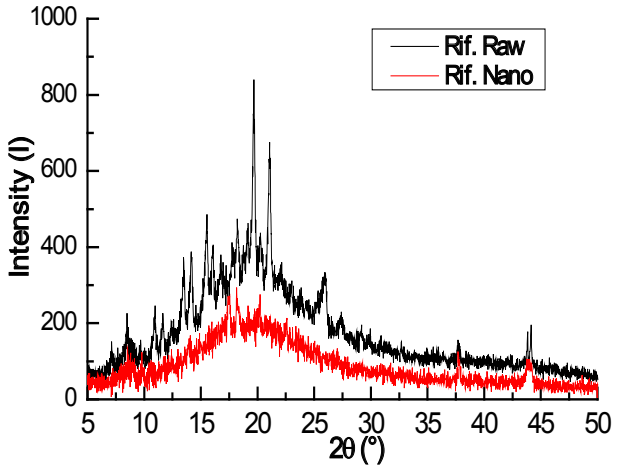

Figure 7: XRD patterns of (a) raw rifampicin and (b) rifampicin nanoparticles. Raw rifampicin shows characteristic peaks at 19.50°, 14.35° and 13.65° and rifampicin nanoparticles presented changes in this pattern, with an amorphous profile.

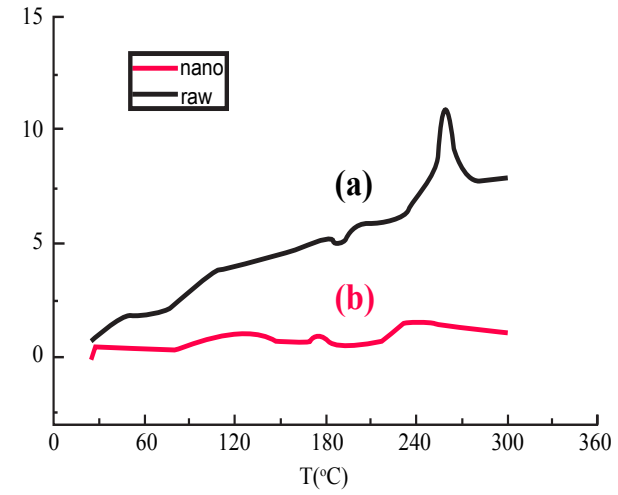

Figure 8: DSC curves of (a) raw rifampicin and (b) rifampicin nanoparticle. Raw rifampicin shows melting point at 190 °C and decomposition at 260 °C. The rifampicin nanoparticles do not present these peaks, showing an amorphous behavior.

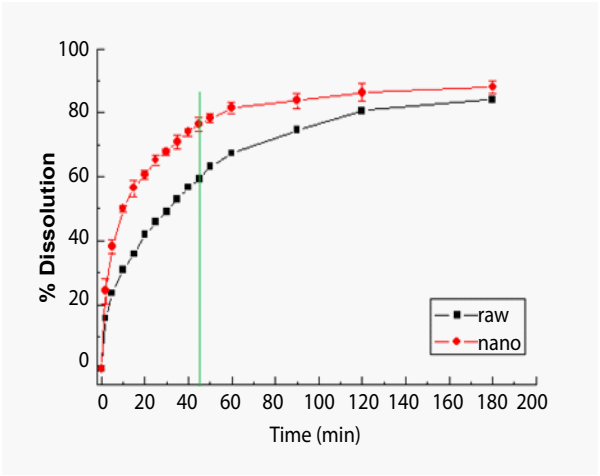

Figure 9: Dissolution rates profile for raw and nano rifampicin in a PBS buffer solution (pH=7.4). The inset shows the dissolution rates for the initial ten minutes.The speed and temperature bath were set at 100 rpm and 37.0 ± 0.5 °C, respectively.

Acknowledgment

The authors would like to thank the CNPq, National Council for Technological and Scientific Development (CNPq), a Brazilian agency of the Ministry of Science, Technology and Innovation (MCTI), for supporting this research (Process Nº 140420/2008). We thank the Laboratory of Magnetic Materials (LMM-IFUSP) for the chromium films deposited by sputtering for the device microfabrication. We thank also the FAPESP founding agency for supporting this work (Process Number: 13/50696-1).

References

1. Shah RK, Shum HC, Rowat AC, Lee D, Agresti JJ, et al. (2008) Designer emulsions using microfluidics. Materials Today 11: 18-27.
2. Chistopher GF, Anna SL (2007) Microfluidic methods for generating continuous droplet streams. J Phys D Appl Phys 40: 319–336.
3. Engl W, Backov R, Panizza P (2008) Controlled production of emulsions and particles by milli- and microfluidic techniques. Current Opinion in Colloid & Interface Science 13: 206–216.
4. Marre S, Jensen KF (2010) Synthesis of micro and nanostructures in microfluidic systems. Chem Soc Rev 39: 1183-1202.
5. Günther A, Jensen KF (2006) Multiphase microfluidics: from flow characteristics to chemical and materials synthesis. Lab Chip 6: 1487-1503.
6. Skurtys O and Aguilera JM (2008) Applications of Microfluidic Devices in Food Engineering. Food Biophysics 3: 1–15.
7. Weng C, Huang C, Yeh C, Lei H, Lee G (2008) Synthesis of hexagonal gold nanoparticles using a microfluidic reaction system. J Micromech Microeng 18: 035019.
8. Jahn A, Reiner JE, Vreeland WN, DeVoe DL, Locascio LE, Gaitan M (2008) Preparation of nanoparticles by continuous-flow microfluidics. J. Nanopart Res 10: 925–934.
9. Merisko-Liversidge E, Liversidge GG, Cooper ER (2003) Nanosizing: a formulation approach for poorly-water-soluble compounds. Eur J Pharm Sci 18: 113-120.
10. Thorat AA, Dalvi VS (2012) Liquid antisolvent precipitation and stabilization of nanoparticles of poorly water soluble drugs in aqueous suspensions: Recent developments and future perspective. Chemical Engineering Journal 182: 1–34.

11. Kawabata Y, Wada K, Nakatani M, Yamada S, Onoue S (2011) Formulation design for poorly water-soluble drugs based on biopharmaceutics classification system: Basic approaches and practical applications. International Journal of Pharmaceutics 420: 1–10.

12. Pouton CW (2006) Formulation of poorly water-soluble drugs for oral administration: Physicochemical and physiological issues and the lipid formulation classification system. Eur J Pharm Sci 29: 278–287.

13. Jahn A, Vreeland WN, DeVoe DL, Locascio LE, Gaitan M (2007) Microfluidic directed formation of liposomes of controlled size. Langmuir 23: 6289-6293.

14. Valencia PM, Basto PA, Zhang L, Rhee M, Langer R, et al. (2010) Single-step assembly of homogenous lipid-polymeric and lipid-quantum dot nanoparticles enabled by microfluidic rapid mixing. ACS Nano 4: 1671-1679.

15. Jahn A, Stavis SM, Hong JS, Vreeland WN, DeVoe DL, et al. (2010) Microfluidic mixing and the formation of nanoscale lipid vesicles. ACS Nano 4: 2077-2087.

16. Karnik R, Gu F, Basto P, Cannizzaro C, Dean L, et al. (2008) Microfluidic platform for controlled synthesis of polymeric nanoparticles. Nano Lett 8: 2906-2912.

17. Panagiotou T, Mesite S, Fisher R, Gruverman I (2007) Production of Stable Drug Nanosuspensions Using Microfluidic Reaction Technology, Proceedings of NSIT-Nanotech 4: 246-249.

18. Desportes S, Yatabe Z, Baumlim S, Génot V, Lefèvre JP, et al. (2007) Fluorescence lifetime imaging microscopy for *in situ* observation of the nanocrystallization of rubrene in a microfluidic set-up. Chemical Physics Letters 446: 212-216.

19. Wanga J, Zhanga Q, ZhouY, Shao L, Chen J (2010) Microfluidic synthesis of amorphous cefuroxime axetil nanoparticles with size-dependent and enhanced dissolution rate. Chem Eng J 162: 844–851.

20. Zhang Q, Xu L, Zhou Y, Wang J, Cheng J (2011) Preparation of Drug Nanoparticles Using a T-Junction Microchannel System. Ind Eng Chem Res 50:13805-13812.

21. Zhao H, Wang JX, Wang QA, Chen FJ, Yun J (2007) Controlled Liquid Antisolvent Precipitation of Hydrophobic Pharmaceutical Nanoparticles in a Microchannel Reactor Ind Eng Chem Res 46: 8229-8235.

22. Zhang QX, Zhou Y, Wang JX, Shao L, Chen JF (2010) Microfluidic Fabrication of Monodispersed Pharmaceutical Colloidal Spheres of Atorvastatin Calcium with Tunable Sizes. Ind Eng Chem Res 49: 4156–4161.

23. Ali HS, York P, Blagden N (2009) Preparation of hydrocortisone nanosuspension through a bottom-up nanoprecipitation technique using microfluidic reactors. Int J Pharm 375: 107-113.

24. Ali HS, York P, Ali AM, Blagden N (2011) Hydrocortisone nanosuspensions for ophthalmic delivery: A comparative study between microfluidic nanoprecipitation and wet milling. J Control Release 149: 175-181.

25. Gumbo T, Louie A, Deziel MR, Liu W, Parsons LM, et al. (2007) Concentration-dependent Mycobacterium tuberculosis killing and prevention of resistance by rifampin. Antimicrob Agents Chemother 51: 3781-3788.

26. Agrawal S, Singh I, Kaur KJ, Bhade SR, Kaul CL, et al. (2004) Comparative bioavailability of rifampicin, isoniazid and pyrazinamide from a four drug fixed dose combination with separate formulations at the same dose levels. Int J Pharm 276: 41-49.

27. Agrawal S, Ashokraj Y, Bharatam PV, Pillai O, Panchagnula R (2004) Solid-state characterization of rifampicin samples and its biopharmaceutic relevance. Eur J Pharm Sci 22: 127-144.

28. Son YJ, McConville JT (2011) A new respirable form of rifampicin. Eur J Pharm Biopharm 78: 366-376.

29. Reverchon E, De Marco I, Della Porta G (2002) Rifampicin microparticles production by supercritical antisolvent precipitation. Int J Pharm 243: 83-91.

30. Changsan N, Chan HK, Separovic F, Srichana T (2009) Physicochemical characterization and stability of rifampicin liposome dry powder formulations for inhalation. J Pharm Sci 98: 628-639.

31. Sung JC, Padilla DJ, Garcia-Contreras L, Verberkmoes JL, Durbin D, et al. (2009) Formulation and pharmacokinetics of self-assembled rifampicin nanoparticle systems for pulmonary delivery. Pharm Res 26: 1847-1855.

32. Álvarez-Castanho M, Ayuso D, Granda M, Fernandez-Abedul M, Garcia J, et al. (2008) Critical points in the fabrication of microfluidic devices on glass substrates. Sensors and Actuators B 130: 436–448.

33. Iliescu C, Chen B, Miao J (2008) On the wet etching of Pyrex glass. Sensors and Actuators A: Chemical 143: 154-161.

34. Rane Y, Mashru R, Sankalia M, Sankalia J (2007) Effect of hydrophilic swellable polymers on dissolution enhancement of carbamazepine solid dispersions studied using response surface methodology. AAPS PharmSciTech 8: Article 27.

35. Junghanns JU, Müller RH (2008) Nanocrystal technology, drug delivery and clinical applications. Int J Nanomedicine 3: 295-309.